# Maximum Power Point Tracking for Permanent Magnet Synchronous Generator based Wind Park Application

R. B. R. Prakash[1‡], P. Srinivasa Varma[1], Ch. Rami Reddy[2], M. Dilip Kumar[3], A. Giri Prasad[4], E. Shiva Prasad[4]

[1]Electrical and Electronics Engineering, Koneru Lakshmaiah Education Foundation, Vaddeswaram, AP, India 522302

[2]Electrical and Electronics Engineering, Malla Reddy Engineering College (A), Secunderabad, Telangana, India 500100

[3]Electrical and Electronics Engineering, St. Peters Engineering College (A), Secunderabad, Telangana, India 500043

[4]Electrical and Electronics Engineering, VNR Vignana Jyothi Institute of Technology (A), Secunderabad, India 500090

(bhanu184@kluniversity.in, pinnivarma@kluniversity.in, crreddy229@mrec.ac.in, manikdilip@gmail.com, giriprasad_a@vnrvjiet.in, shivaprasad_e@vnrvjiet.in)

‡Corresponding Author: R. B. R. Prakash, bhanu184@kluniversity.in

*Received: 12.03.2022 Accepted: 02.05.2022*

**Abstract-** The world's energy consumption is constantly growing, and conventional energy sources may soon be depleted. Wind energy is one such discovered new energy source that is abundant and renewable. However, induction generators require large excitation capacitors and bi-directional power flow controllers. Permanent magnet synchronous generators are now more appropriate for variable speed Direct Driven Wind Power Conversion Systems (DDWPCS). Earlier, a three-stage power conversion for variable ac voltage was done. To reduce these power conversion stages and to overcome the limitations of conventional systems, the Z-Source Inverter (ZSI) based Direct Drive Wind Energy Conversion Systems (DDWECS) is introduced. Mathematical modelling equations are derived for various operating modes of operation using ZSI. In the proposed method Space Vector Pulse Width Modulation (SVPWM) & Modified SVPWM (MSVPWM) methods were compared for shoot through period placement, voltage gain, and Total Harmonic Distortion (THD). The MSVPWM places the shoot through period faster and also it reduces input current THD by 3.6% and output voltage THD by 7.8%. Also, this adds a PWM controller to suppress 3rd order harmonics. To validate the proposed ZSI, simulation is carried out in MATLAB and the results are tabulated.

**Keywords**-Wind energy conversion system; Permanent magnet synchronous generator; Z- Source inverter; Space vector pulse width modulation; Modified space vector pulse width modulation.

**Nomenclature**

| | |
|---|---|
| DDWPCS | Direct Driven Wind Power Conversion Systems |
| ZSI | Z-Source Inverter |
| PWM | Pulse Width Modulation |
| SVPWM | Space Vector Pulse Width Modulation |
| MSVPWM | Modified Space Vector Pulse Width Modulation |
| THD | Total Harmonic Distortion |
| WECS | Wind Energy Conversion System |
| PMSG | Permanent Magnet Synchronous Generator |
| HCS | Hill climbing search |
| HCSC | Hill climbing search control |
| DFIG | Doubly Fed Induction Generator |
| MPPT | Maximum Power Point Tracking |
| PSO | Particle Swarm Optimization |
| VSI | Voltage Source Inverter |
| MBC | Maximum boost control |
| THI | Third Harmonic Injection |
| $\rho$ | Air density |
| A | blade area |

| | |
|---|---|
| $V_W$ | wind velocity |
| P | Power |
| R | Radius of the turbine blade |
| $C_p$ | Power coefficient |
| $\lambda$ | Tip Speed Ratio |
| $T_e$ | Electromagnetic Torque |
| $L_m$ | mutual inductance |
| $i_{qs}$ | q-axis stator current |
| $i_{ds}$ | d-axis stator current |
| $i_{qr}$ | q-axis rotor current |
| $i_{dr}$ | d-axis rotor current |
| $R_s$ | Stator Resistance of PMSG |
| $L_s$ | Inductance of PMSG |
| E | Generated voltage of PMSG |
| $V_t$ | terminal voltage of PMSG |
| *i* | PMSG stator current |
| $i_q$ | q-axis stator current of PMSG |
| $i_d$ | d-axis stator current of PMSG |
| $\psi_q$ | q- axis flux linkages |
| $\psi_d$ | d- axis flux linkages |
| $V_c$, $V_{c1}$, $V_{c2}$ | Capacitor voltages |
| $V_L$, $V_{L1}$, $V_{L2}$ | Inductor voltages |
| $V_{DC}$ | DC Voltage |
| $V_i$ | Inverter voltage |
| $V_m$ | peak voltage |
| $V_{ac}$ | ac output voltage of ZSI |
| B | Boost factor |
| G | Voltage gain |
| M | Modulation index |
| D, $D_0$ | shoot through duty ratios |

## 1. Introduction

With the ever-increasing demand for electrical energy and our serious concern over environmental pollution, the generation of power from wind is attracting attention. The fixed speed wind energy conversion system requires a gearbox for regulating its speed, terminal voltage and supply frequency. A gearbox system increases the conversion loss and aerodynamic noise and decreases the efficiency. In addition, it requires considerable maintenance. Recent advancements in power electronics equipment have widened the scope for installing the variable speed WECS. Although conventional type induction generator has the advantages of robust construction and maintenance free operation, it has drawbacks like low power factor and it requires an ac excitation source. Due to the low cost of the permanent magnet materials, the PMSG brings the variable speed WECS into the market for multi megawatt wind turbine applications.

In the literature survey, it has been found that conventional induction generators and alternators are not suitable for WECS, as they suffer from low torque and low efficiency. To overcome this problem direct drive WECS using PMSG is proposed. This scheme does not require any gearbox, it is easy to control, smaller in size and weight, and has much higher efficiency. The three stages of the conventional power converters are subject to more switching stress consequently more switching losses and the corresponding maintenance. Cost effective design of variable speed WECS using PMSG for a speed range of 20 rpm to 200 rpm is presented in [1]. Radial flux PMSG called torus was presented in [2]. Many researchers have discussed three stage of power converter for WECS. The common drawback of these traditional three stage power conversion systems was discussed [3]. To get the constant voltage by adjusting the duty cycle of a boost chopper was presented in [4]. The dead time in the inverter output reduces the power quality of the dc output voltage which requires a large value of LC in the filter, in addition, they are vulnerable to noise [5]. PWM inverter imposes high switching stress on the switching devices [6]. To suppress the above problem, large size LC filters were suggested by them. The problem of a conventional three stage dc-dc-ac conversion system was presented in [7]. They have proposed a high buck boost DC-AC ZSI. [6] Presented a two constant boost control method for ZSI. But they did not take into account the problem of THD. The reference [8] presents a ZSI which greatly enhances the reliability of the inverter. In [9] the modified space vector for ZSI. The shoot through placement in the space vector of zero states is not uniform and hence switching stress is more. A novel 1-φ Z-source multilevel inverter is proposed in [10]. They used the diode clamped topology but this topology increases the complexity of complex circuits. [2] Had discussed the P and O algorithm-based MPPT controller in which the speed is variable in steps and the power utilized by the MPPT is reached. [11] Proposed HCSC method for MPPT controllers of WECS. [12] Described a method to solve the tracking speed versus control efficiency problem by HCS. The design of a wind turbine system with the usage of DFIG as the power generating system which can be operated in grid-connected mode or in grid disconnected mode is presented in [13].

A grid connected qZSI Photovoltaic power system is presented in [14]. They have designed a DC link voltage controller and AC side power controller for improving the performance of qZSI-based photovoltaic systems. A modified NLMS-based control algorithm is designed to control the distributed generation system feeding three phase nonlinear loads. The control algorithm extracts the fundamental weight components with reduced oscillations from the load current [14]. To extract maximum power for a

hybrid solar-wind renewable energy system using the PSO for standalone applications is presented in [15]. Maximum power extraction based on PSO works to achieve optimal power on HRES by adjusting the duty cycle for the boost converter for each energy source system based on current and voltage measurements.

But the authors have not considered frequency variations of DC link voltage concerning photovoltaic voltage variations and also the DC link voltage controller requires a complex control algorithm. A qZSI derived from the traditional ZSI is presented in [15]. The qZSI features a wide range of voltage gain which is suitable for applications in photovoltaic systems. To enhance the performance of qZSI, the authors have proposed design guidelines for boost control methods. Even in that case, the efficiency is not improved and the cost of qZSI is not reduced when compared with traditional ZSI. To circumvent the limitations of the traditional ZSI, qZSIs was proposed [18]. It reduces passive component ratings and improves input profiles. The consistent DC makes qZSI suitable for PV applications [18]. Advanced dc-dc converter improvement techniques such as Switch Capacitor (SC), Switch Inductor (SL) and hybrid SC/SL technology have been disclosed recently to increase the boost factor of the traditional ZSI. So ZSI and Switch inductor are combined to produce a high boost factor. This includes constant current from the input DC source, reduced component ratings, and improved dependability [20]. In the last decade, the fixed-speed wind energy conversion system has given way to variable-speed systems due to their poor energy extraction, mechanical stress on moving parts and poor power quality. Mechanical stress and aerodynamic noise have been minimized by these variable-speed devices [21]. They can be regulated to allow the turbine to work in a wide range of wind velocities at its optimum power coefficient, obtaining greater wind energy collection with instant response to wind velocities and load changes [21], [22] and energy capture from the wind. The gearless wind system also allows optimum energy yield and minimal costs to be achieved, as reported by [23-26]. According to the electric machine design principles, the wind energy conversion system at fluctuating speeds requires a very bulky generator with a large number of poles [27]. Fig. 1 shows the wind turbine generator with and without gearbox topology. To be easily mounted at the top of the tower and directly connected to the wind turbine, the type of generator for this application must be compact and lightweight.

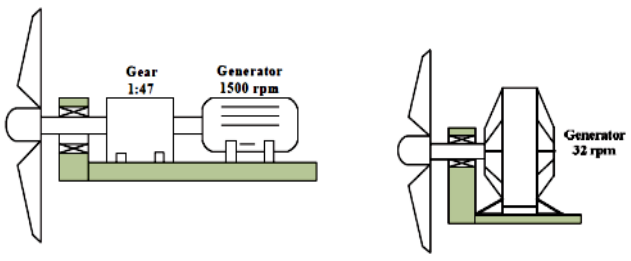


**Fig 1**. Types of wind turbine generators (a) With gearbox and (b) Without a gearbox

This work deals with DDWECS. For direct-driven generator needs a very low-speed operation to match the wind turbine speed and at the same time, to produce electricity in a normal frequency range [28]. The recent development in power electronic devices and its control strategy over energy-efficient DDWECS has aroused interest in using PMSG in small and medium DDWECS. There are three phases in traditional to achieving the required voltage and frequency, power conversion systems interface circuits such as the rectifier, dc-dc boost chopper and PWM inverter [28]. VSI and the PWM are commonly used in WECS to get AC, but it has the disadvantages of needing a dc to dc boost chopper to get a constant dc voltage of higher amplitude [29]. Conventional three stages of power conversion require bulky DC link inductor and capacitor, Electrical decoupling between the generator and the grid is provided by the intermediate DC connection [31]. Therefore, the compensation of accumulated kinetic energy in a wind turbine requires a separate controller. The use of PMSG has been documented in some literature. The proposed ZSI [32] and the traditional DDWECS overcome the limitations of PWM-VSI. It is a single stage dc-ac converter buck-boost and thus its performance is improved over the conventional WECS [33-35]. With this ZSI the boost chopper is removed without any change in the objectives. [35] Presented the ZSI enables short circuits through every phase leg and thus improves the efficiency of the system.

The main contributions and novelty of this work can be summarized as follows:

- The ZSI is proposed as a power conditioner in DDWECS to reduce the number of power conversion stages to two as against three in the conventional system.
- The ZSI features buck-boost capability due to an extra shoot-through state created in the zero state of the typical inverter pulse width modulation. The shoot-through condition is used to enhance the input voltage. The shoot-through pulse width is adjusted as per the PMG generated voltage level to maintain constant load voltage.
- The presented study emphasizes investigating the two PWM control methods such as carrier-based third harmonics control and modified space vector PWM are employed to analyze the performance of the Z-source inverter. The two independent control variables such as shoot-through duty ratio and modulation index are suitably adjusted to get the required voltage and power.
- To improve the system performance, sensor less MPPT controller is incorporated into the system is introduced to avoid conventional sensors. Using this scheme the generator speed required for the existing wind velocity to generate maximum power is predicted.

Text in the paper is presented as follows: Section II describes the proposed ZSI based DDWECS and also gives the

operating modes of the proposed system, Section III describes the control strategy of the proposed converter, Section IV and Section V discusses the performance analysis and presents the results of simulation and discussion for various inputs and outputs of the proposed MPPT controller with ZSI conditions of the proposed converter concerning voltage gain, switching stress, input, output and THD. Lastly, section VI presents the conclusions.

## 2. Proposed ZSi Based Ddwecs

Using three stages of power conversion, the power conversion was done earlier to obtain variable ac voltage at variable frequency. DDWECS-based ZSI is implemented to reduce the power conversion stages and to overcome the limitations of traditional systems. With the assistance of mathematical equations, the ZSI's operating modes with DDWECS are addressed. It gives and describes in detail the mathematical equations for boost factor, voltage gain and switching stress. The two-stage power conversion method by integrating the ZSI for DDWECS is shown in Fig. 2. Here, without any change in aims, the ZSI replaces the buck raise chopper. The ZSI enables the short circuit to increase system reliability at every stage leg. Fig. 3 shows the full circuit of the proposed WECS with ZSI. The PMSG output is fed through its stator inductances and resistances and then to the rectifier [11]. The rectifier serves as the DC supply and its output is given as input to the ZSI.

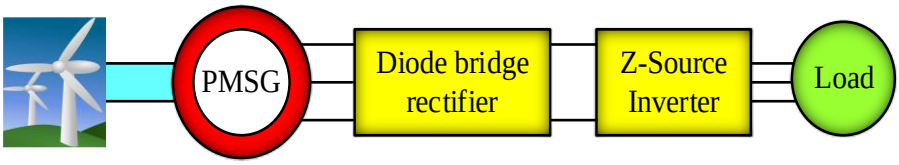


**Fig 2**.DDWECS with two stage power conversion

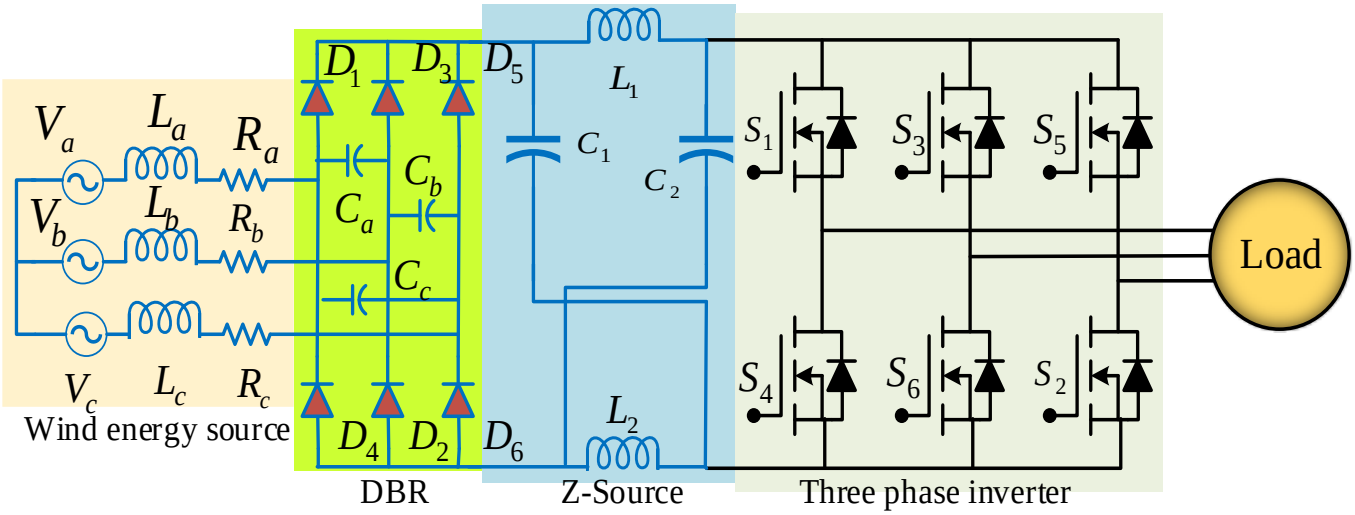


**Fig 3.** PMSG with Z-Source inverter and rectifier

Any VSI can be operated in eight different switching modes, out of which six are said as active states and the remaining two are termed as zero states or modes. As here ZSI is integrated, it offers one more additional state of operation; the ninth state is named as shoot-through zero state. In these operating states two switches on the same limb or any two legs made ON, it causes the load terminals to short circuit. This ninth state 'shoot-through zero state', adds a buck boost special provision to the inverter [11]. Switching intervals of the ZSI are shown in Table 1. Here the appreciable objective of the ZSI is its actions to generate any desired output voltage based on the grid code requirements [12]. Modeling and analysis of the proposed converter are discussed in the next section.

### *A. Modeling of Wind Turbine and PMSG*

The wind turbine and permanent magnet generator mathematical equations are generated, modeled and simulated in MATLAB.

#### *A.1. Wind Tturbine Model*

The wind is just air moving, air has mass despite its low density. The kinetic energy of wind is related to the mass times the square of the wind velocity. The mass of air traveling in time is the combination of air density ( $\rho$ ), blade area (A) and wind velocity ($V_W$).

The kinetic energy in the region

$$P = \rho A V_w^3$$

The amount of energy collected by a wind turbine is provided by the

$$P = 0.5\pi R^2 V_W^3 \rho C_P$$

Where

$\rho$ = Air density

R = Radius of the turbine blade (m)

$V_w$ = Wind velocity (m/s)

$C_p$ = Power coefficient

The $C_p$ curve will be approximated analytically using Eq. (1) CP has a theoretical top value of 0.59, although in practice it ranges from 0.2 to 0.4.

$$C_P = \frac{16}{27}\lambda\left[\lambda + \frac{1.32 + \left(\frac{\lambda - 8}{20}\right)^2}{\beta^{2/3}}\right] - \frac{0.57\lambda^2}{\frac{C_1}{C_d}\left[\lambda + \frac{1}{2\beta}\right]} \quad (1)$$

Fig 3. shows a basic way to represent a wind turbine. eq shows the generating torque in an arbitrary reference frame (2).

$$T_e = \left(\frac{3}{2}\right) * \left(\frac{P}{2}\right) * L_m\left[i_{qs} i_{dr} - i_{qr} i_{ds}\right] \quad (2)$$

### *A.2. Permanent Magnet Synchronous Generator*

An accurate machine model is required to predict PMSG steady state and transient behavior. The model should find the machine's dynamic reaction. The dynamic model accounts for changes in voltage, current, stator frequency, and torque. It is generated utilizing a two-phase machine on the direct and quadrant axis.

$$E = V_t + iR_s$$

$$V_t = L_s \frac{di}{dt} - iR_s$$

$$V_t = \lambda\psi - iR_s$$

The d and q axis voltages are as follows.

$$V_q = -R_s i_q + \frac{d}{dt}\psi_q$$

$$V_d = -R_s i_d + \frac{d}{dt}\psi_d$$

Eq. (3) gives the electromagnetic torque in the rotor reference

$$T_e = \left(\frac{3}{2}\right) * \left(\frac{P}{2}\right) * \left[\psi_d i_q - \psi_q i_d\right] \quad (3)$$

Where P= Number of poles

### *B. Operating Modes of Proposed ZSI*

The proposed system operates in three different modes as follows.

**Mode-1:** Fig. 4 demonstrates ZSI's equivalent circuit for operation in mode-1. In one of the two traditional zero states, the inverter bridge operates and short-circuits either the upper or lower three devices. It, therefore, functions as an open circuit perceived from the network of Z-source. The PMSG phases a and b are linked via the two diodes to the impedance network. Diodes D1 and D6 are in series with capacitor Ca.

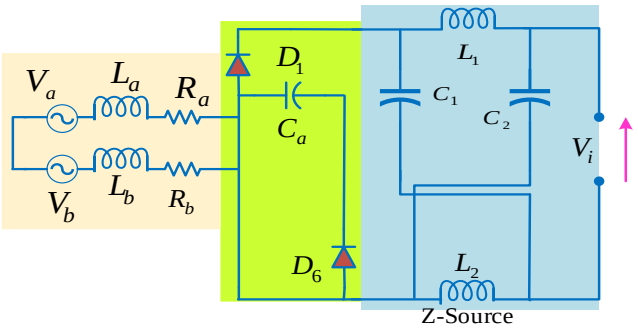


**Fig 4**. Equivalent circuit of ZSI for mode-1

**Mode-2:** The ZSI equivalent circuit in shot through service is shown in Fig. 5. In this mode, both diodes are OFF due to higher voltages in inductors, separating the dc connection from the ac line. The PMSG is thus disconnected from the load. In any switching cycle during the traditional zero states created by the PWM control, this shoot-through mode can be used. Based on the appropriate boost factor, the shoot through time or shoot-through duty cycle is calculated using Eq. (13).

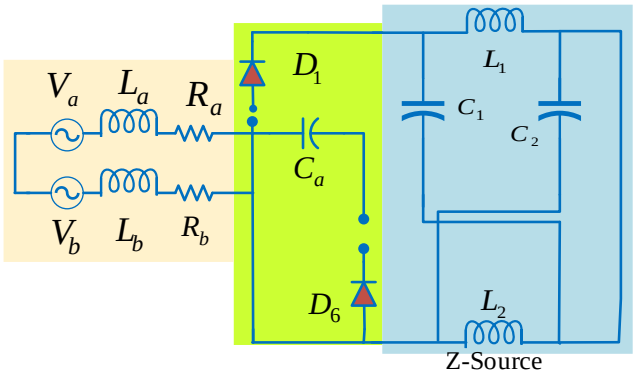


**Fig 5**. Equivalent circuit of ZSI for mode-2

From the Fig. 5 the voltage across capacitor is Eq. (4)

$$V_{C1} = V_{C2} = V_C \quad (4)$$

The voltage across inductor Eq. (5)

$$V_{L1} = V_{L2} = V_L \quad (5)$$

When the shoot-through period ($T_0$) is accommodated during the switching period T, the capacitor and the inductor voltages are equal as in Eq. (6).

$$V_L = V_C \tag{6}$$

The voltage input to the Z- source circuit is given as Eq. (7)

$$V_{DC} = 2V_C \tag{7}$$

The voltage across Inverter Bridge is of Eq. (8)

$$V_i = 0 \tag{8}$$

**Mode-3:** Fig. 6 shows the ZSI equivalent circuit in typical active state operation. In this mode, an inverter bridge can be run in each of the six historically active states. The voltage during this state is impressed by the load.

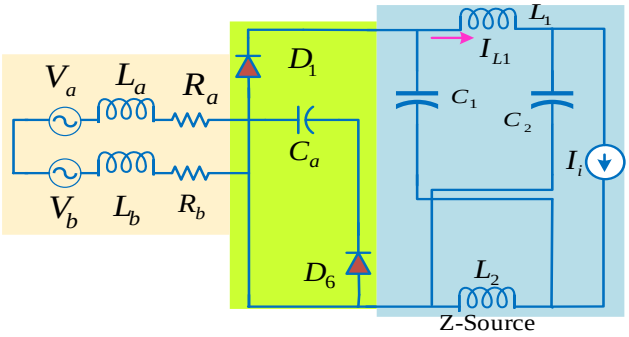


**Fig 6**. Equivalent circuit of ZSI for mode-3

The voltage across the inverter when the active time ($T_1$) is accommodated within the switching period (T) is given by Eq. (9)

$$V_i = V_{DC} - V_C \tag{9}$$

The voltage acquired after input of the Z-source circuit to the inverter bridge is Eq. (10)

$$V_i = 2V_C - V_{DC} \tag{10}$$

The average voltage over the one switching time (T) across the inductor is equal to zero as in Eq. (11).

$$V_L = 0 \tag{11}$$

The input voltage for the inverter circuit is expressed as Eq. (12)

$$V_i = B\frac{V_{DC}}{2} \tag{12}$$

Where,

B is Boost factor and is give by, $B = \dfrac{1}{1-2D_0}$

$D_0$ is the shoot through duty ratio, $D = \dfrac{T_0}{T}$

Rectifier output voltage is given by Eq. (13)

$$V_{DC} = \frac{3\sqrt{3}}{\pi}V_m \tag{13}$$

Eq.(9) can be rewritten as Eq. (14)

$$V_i = \frac{3\sqrt{3}}{2\pi}V_m B \tag{14}$$

The rms output voltage of the ZSI can be expressed as Eq. (15)

$$V_{ac} = \frac{3\sqrt{6}}{2\pi}V_m G \tag{15}$$

where G is voltage gain

***Implementation of PWM Schemes for ZSI***

The same PWM algorithms for VSI may be utilized for ZSI with minor adjustments. The shoot-through period distribution in the switching waveforms of the standard PWM concept controls the output voltage of ZSI [8]. The controllable ac output voltage, voltage stress across switching devices, and the harmonic profile of the ac output characteristics are all dependent on how the control algorithm inserts the shoot-through period. Several control strategies have been proposed in recent years. There are two main types of MBC: THIPWM and MSVPWM. Fig. 7 displays the maximum boost control PWM technique with THI control. In this PWM method, the three-phase reference voltages are injected with a 1/6th harmonic component of the fundamental component. The R phase $V_r$ peaks at 3/2 M, while the Y phase $V_y$ peaks at -3/2 M. Thus, two straight lines, $V_p$ and $V_n$, regulate the shot through time with 16% third harmonic injection. The shoot-through pulses' amplitude and breadth vary with PMSG voltage fluctuations.

The maximum shoot through duty ratio obtained by this scheme can be written below

$$D_0 = \frac{2\pi - 3\sqrt{3\pi}}{2\pi}$$

Important expressions in this PWM method are given below:

Voltage Gain, $G = M\left(\dfrac{1}{1-2D_0}\right)$

Modulation Index, $M = \dfrac{\pi G}{3\sqrt{3G-\pi}}$

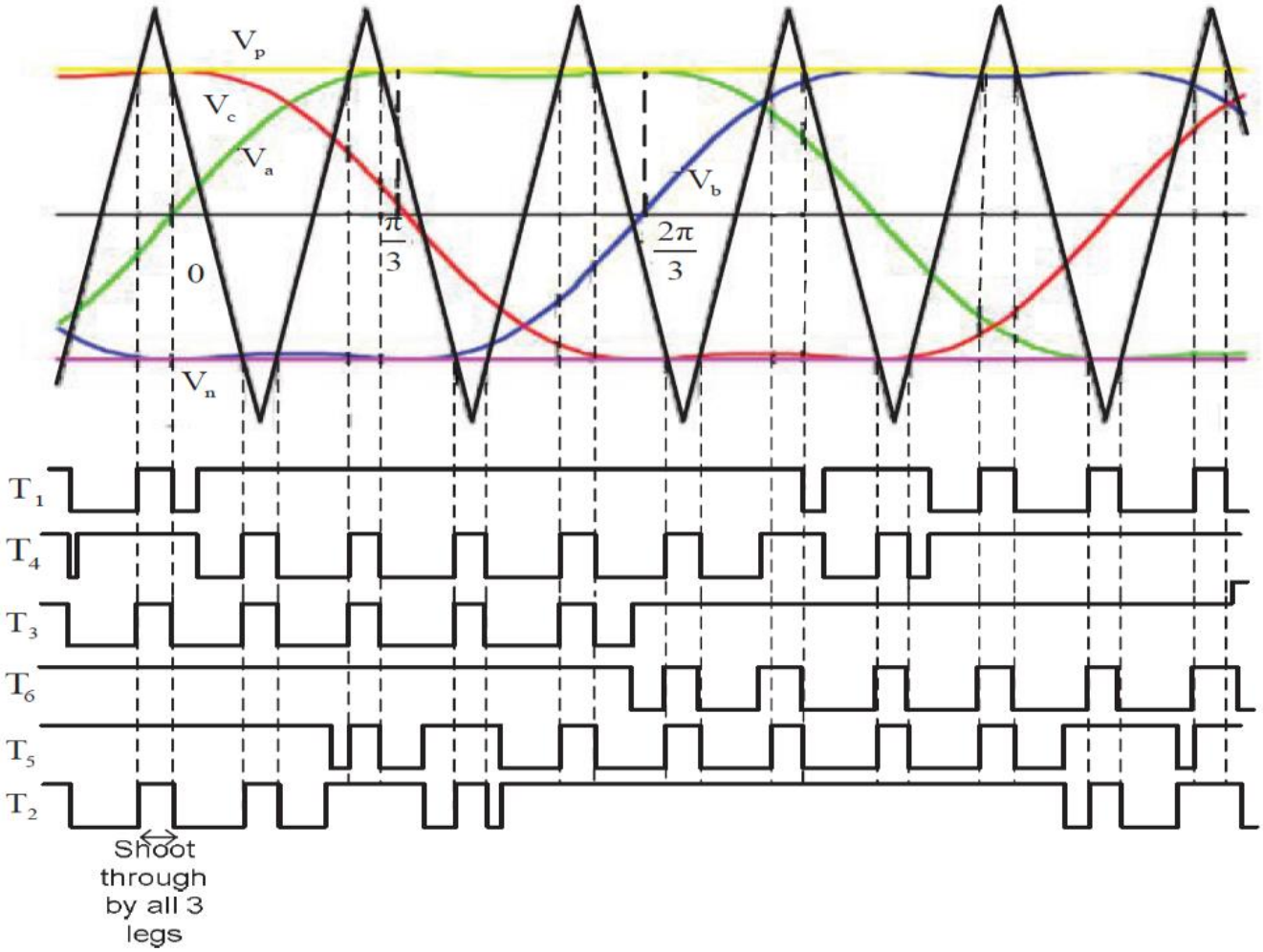


**Fig 7.** Carrier based PWM Scheme with third harmonic injection

Boost Factor, $$B = \frac{3\sqrt{3G - \pi}}{\pi}$$

The ac output voltage of the ZSI with this scheme is given as

$$V_{ac} = \frac{9\sqrt{6}}{2\pi} * \frac{\sqrt{3M.B - \pi}}{\pi} V_{rms} M$$

Where $V_{rms}$ is per phase PMSG generated voltage

## 3. Control Strategy of Proposed Topology for Mppt Implementation

To achieve better performance of AC line voltage control of ZSI and PMSG generated voltages are sensed and compared to predefined reference values. The boost factor is determined by the time duration of the shoot and the desired output voltage. The boost factor is the control variable of the ZSI voltage and the modulation index for that of load voltage. The complete controller block diagram for a DDWECS with PMSG and ZSI is shown in Fig. 8. During fluctuating voltage conditions, the ZSI DC connection voltage is modified by periodic shoot insertion through states following the PMSG generated voltage. Based on the PMSG voltage variations via the voltage feedback loop, the control of dc connection voltage is carried out. The DC connection voltage is calculated and compared in this mode and error is processed to change the shooting period by state. The modulation index and the boost factor that relies on the shoot through time inserted in the traditional switching waveform are the two parameters to be adjusted to get the desired output AC voltage in the ZSI.

## 4. Results and Discussion

This section describes the MATLAB/ SIMULINK tool used to model the horizontal axis wind turbine and permanent generator equations. At a cut in wind velocity of 3m/s, the direct-drive permanent magnet generator begins to create electricity and ceases at a cutout wind velocity of 12m/s. Fig. 9 depicts the relationship between turbine speed and time for different wind speeds.

Fig. 10 shows the simulated waveforms of wind turbine speed and produced voltage for various values of wind velocity. 116 rpm @ 6m/s, the wind turbine generator generates 182 Volts from the permanent magnet generator due to the rotor's increased number of poles. At a wind speed of 10m/s, the voltage is 275V. At 3m/s and 10m/s, the produced voltage has a frequency of 7Hz and a maximum of 25Hz, respectively

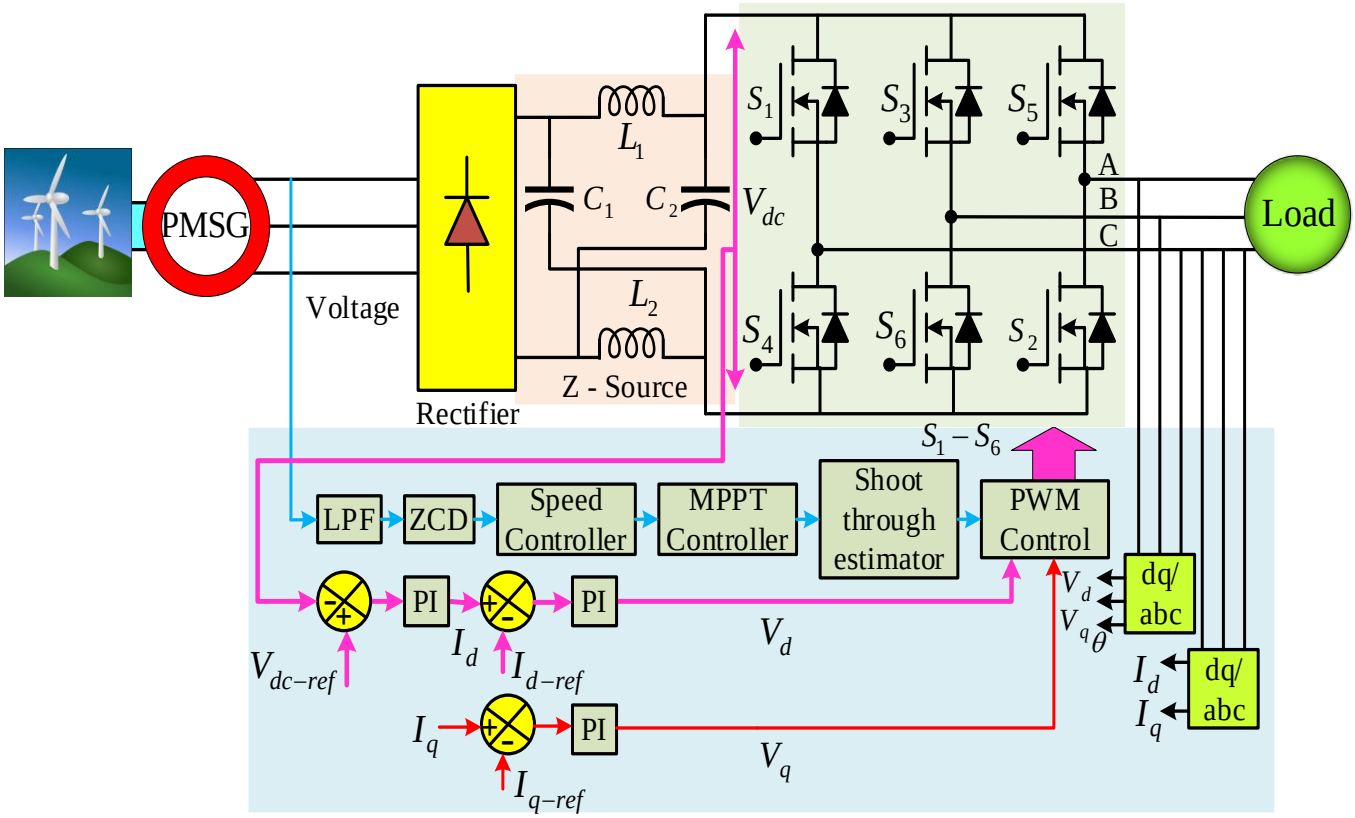


**Fig 8.** Control strategy of ZSI- DDWECS for MPPT implementation

In the MATLAB/SIMULINK program, the two-stage power converter, which consists of the rectifier, the ZSI, and the MPPT sensor less controller, is modeled and simulated. When different wind speeds were used, the model was simulated and the results were examined. The results of the simulations for various wind velocity settings are shown in Table. 1, for reference. It is clear from the table that the PMSG cannot capture the whole power spectrum. The amount of energy derived from wind grows in tandem with the increase in wind velocity. The entire power of the wind turbine, on the other hand, cannot be produced without the use of the MPPT controller.

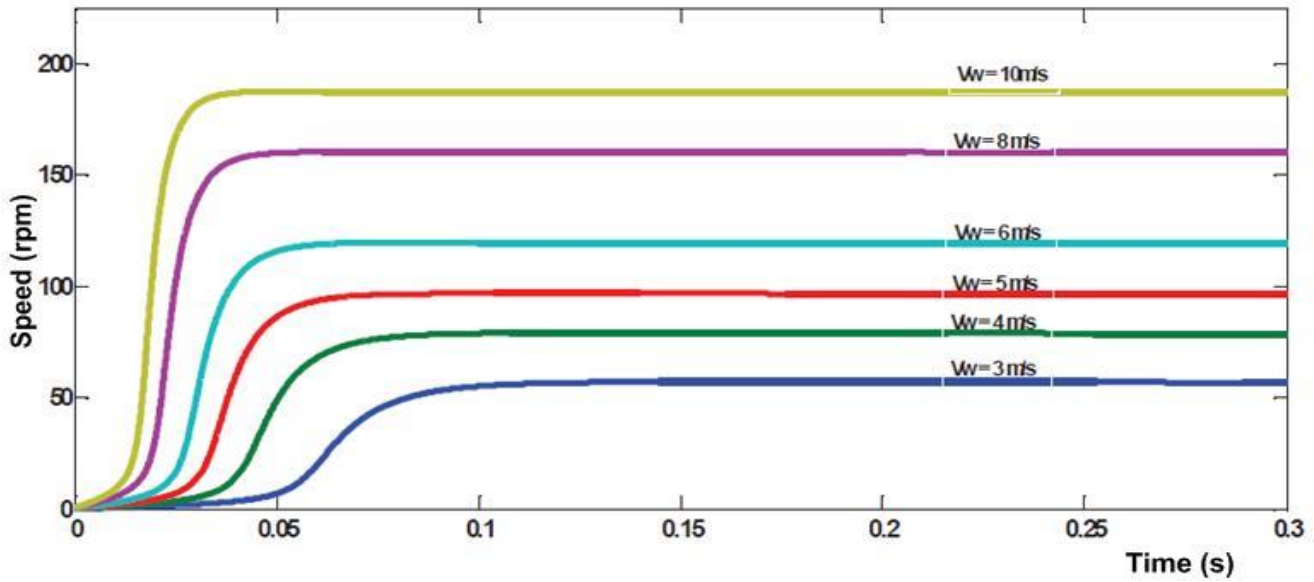


**Fig 9**. Wind turbine speeds for various wind velocity conditions

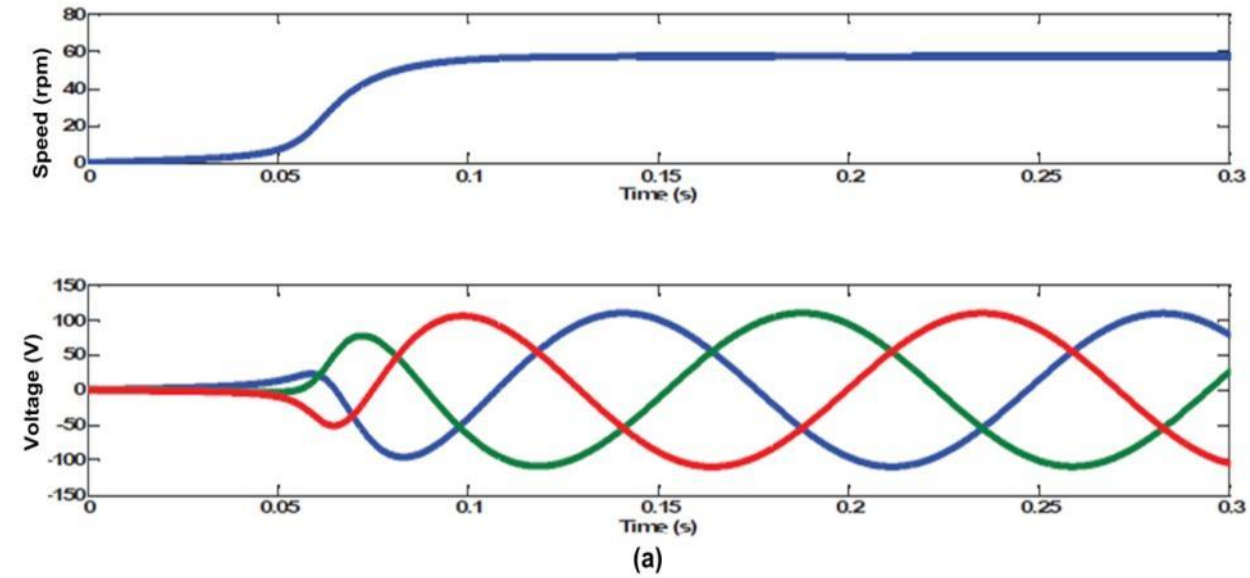
Speed (rpm)
Time (s)
Voltage (V)
Time (s)

(a)

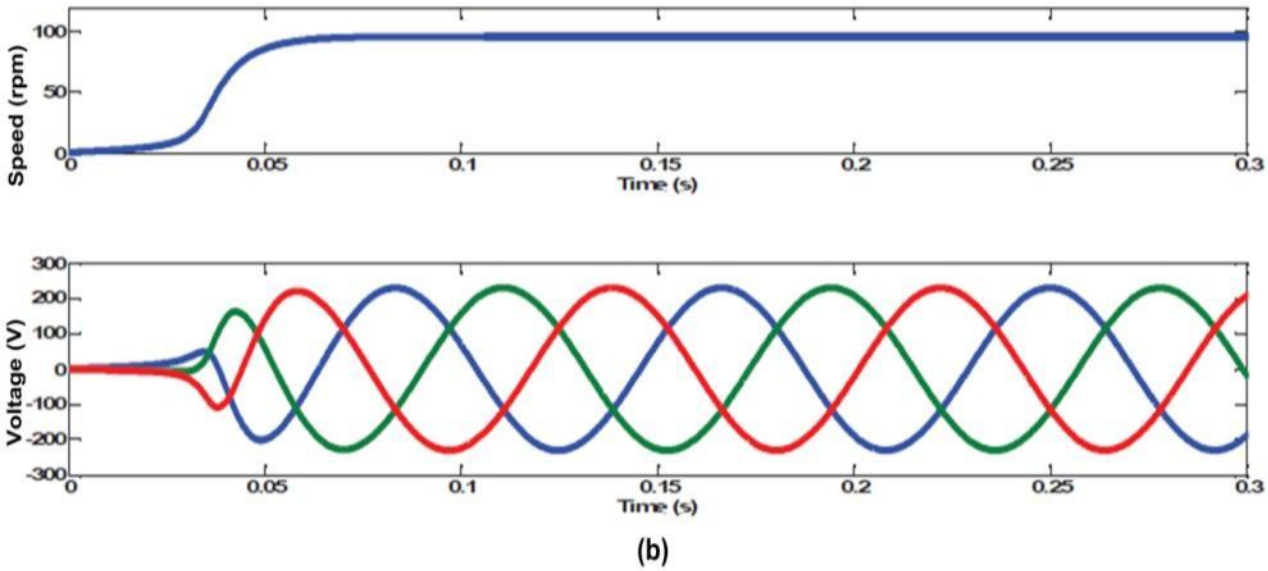
Speed (rpm)
Time (s)
Voltage (V)
Time (s)

(b)

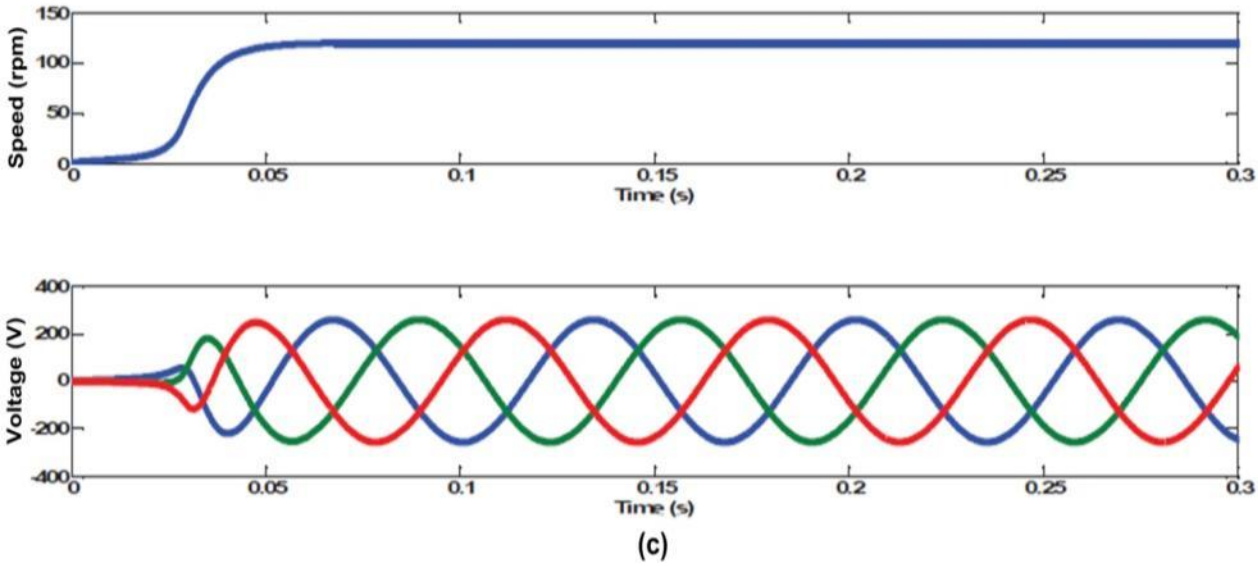
Speed (rpm)
Time (s)
Voltage (V)
Time (s)

(c)

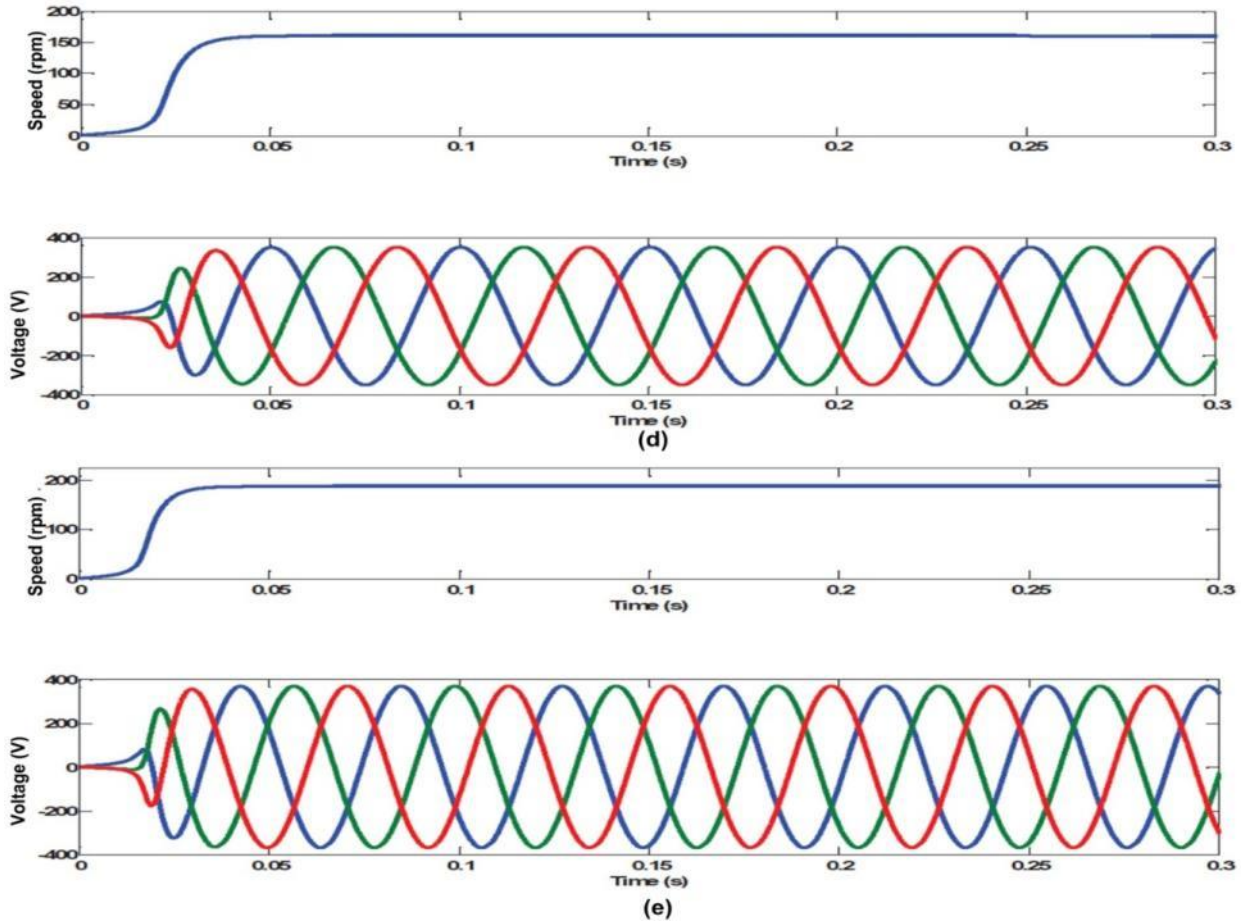


**Fig 10**. Simulated waveforms of turbine speed and PMSG generated voltage for wind velocity of (a) 3m/s (b) 5m/s (c) 6m/s (d) 8m/s (d) 8m/s and (e) 10m/s

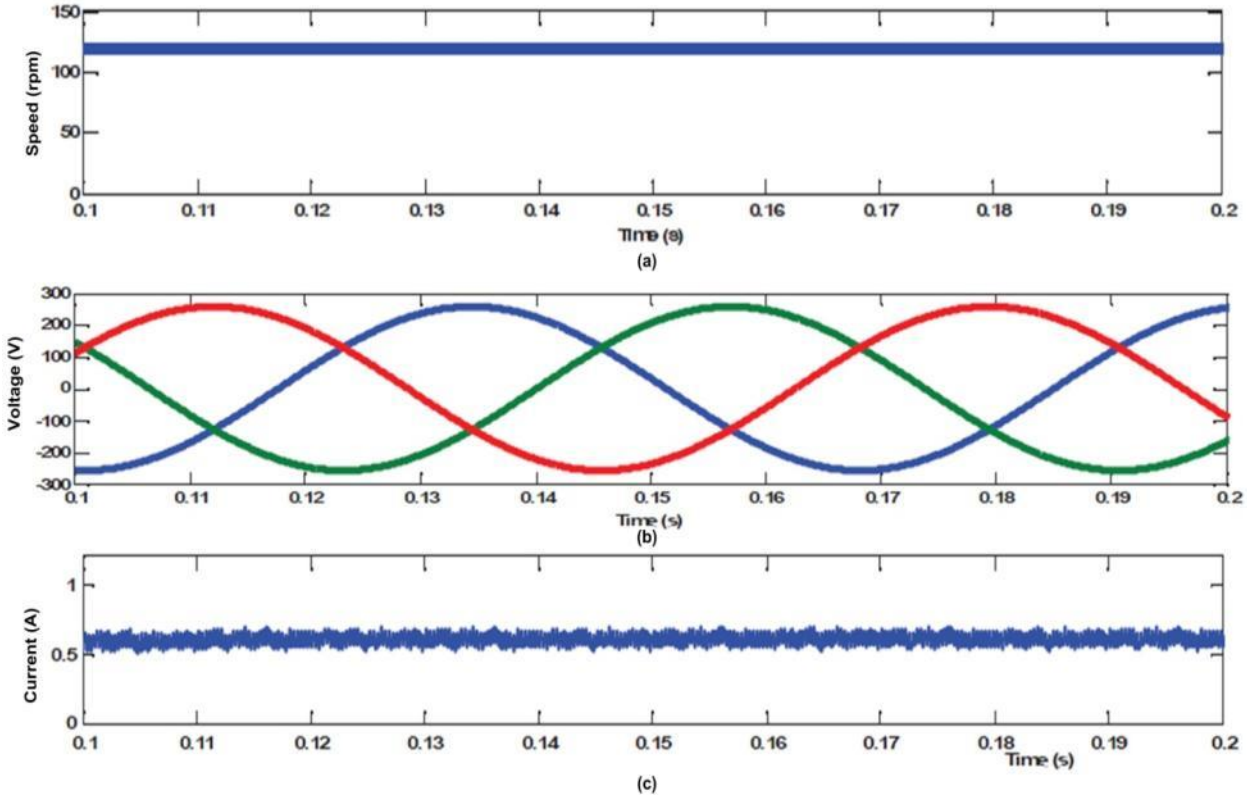

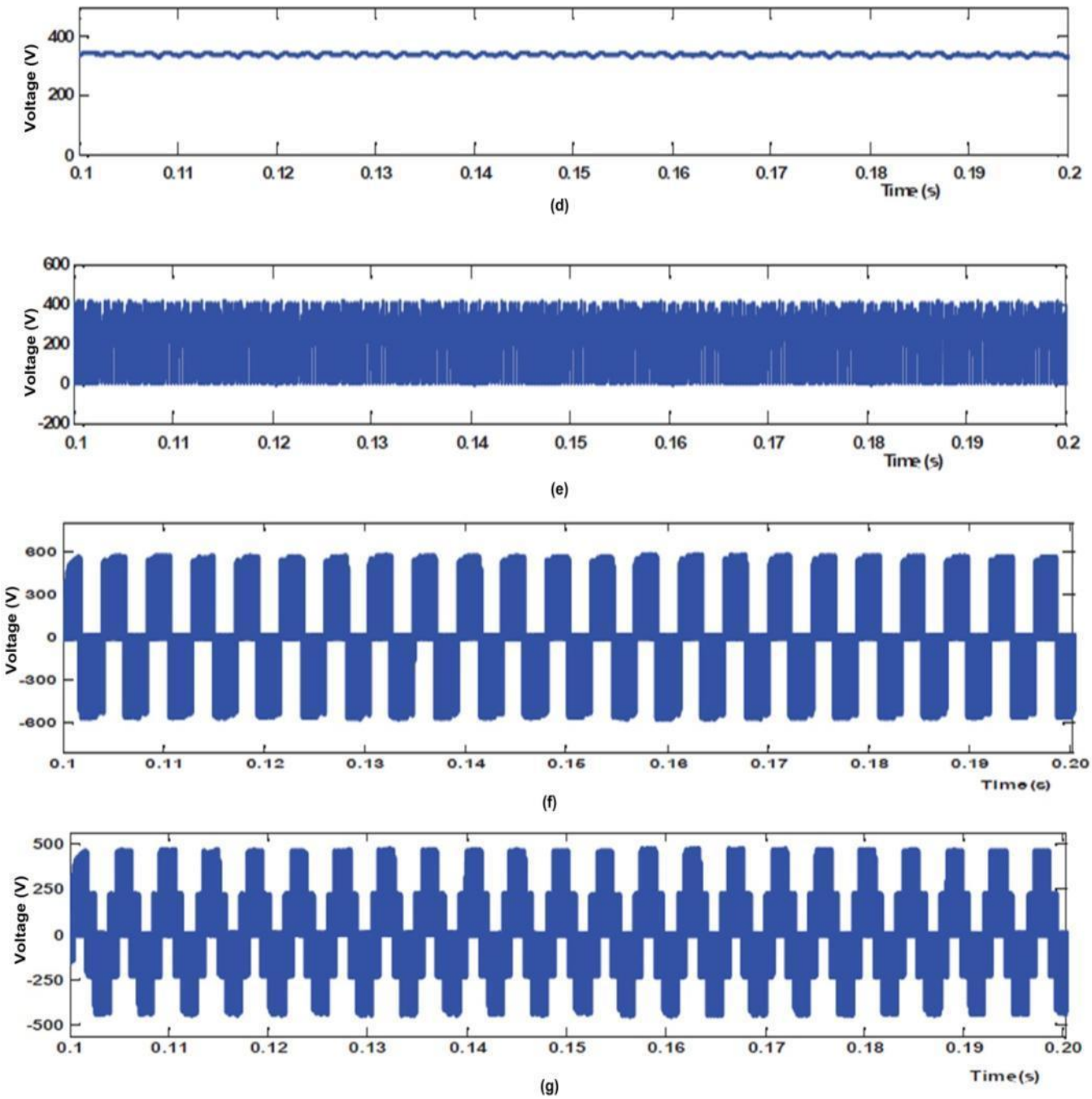


**Fig 11**. Simulated results of proposed DDWECS with ZSI controlled by THIPWM Scheme (a) Wind turbine speed (b) PMSG generated voltage (c) Inductor current (d) Capacitor voltage (e) DC link voltage (f) Line voltage and (g) Phase voltage

Fig. 11 shows the simulated waveforms of the proposed DDWECS with ZSI controlled by the THIPWM scheme. The model is simulated for a wind velocity of 6m/s turbine speed of 116rpm, generated voltage of 182 Volts, the load of 0.5kW shoot through duty ratio of 0.3 and modulation index of 0.7. The DC line voltage of 400V obtained for the input voltage of 182V AC with a shoot through duty ratio of 0.3 is as shown in Fig. 11(e). ZSI is controlled by modified space vector pulse width modulation to predict its performance which is analyzed for a wind velocity of 6m/s and generator speed of 116rpm and generated voltage of 182V. The shoot through duty ratio $D_0$ 0.3 and modulation index M 0.7 are selected to obtain the desired value of space vector pulses for ZSI.

The shoot through placement in the zero states is varied according to PMSG generated voltage. Fig. 12 (c) to Fig. 12 (e) show the inductor current, capacitor voltage and DC link voltage waveforms respectively. When compared with the THIPWM scheme the voltage and current ripples magnitude are reduced and hence switching voltage stress is reduced significantly.

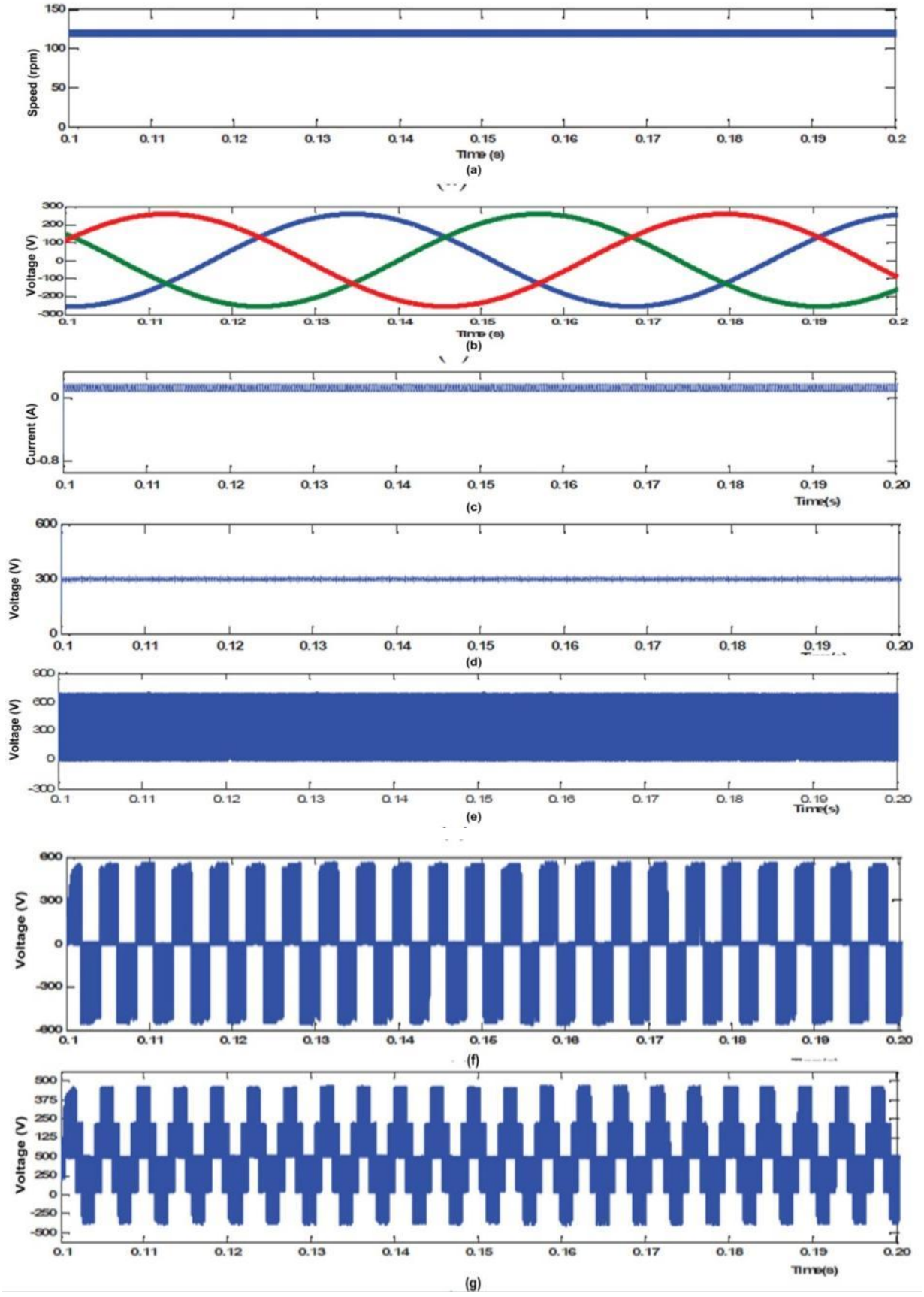


**Fig 12**. Simulated results of proposed WECS with ZSI controlled by MSVPWM scheme (a) Wind turbine speed (b) PMSG generator voltage (c) Inductor current (d) Capacitor voltage (e) DC link voltage (f) Line voltage and (g) Phase voltage

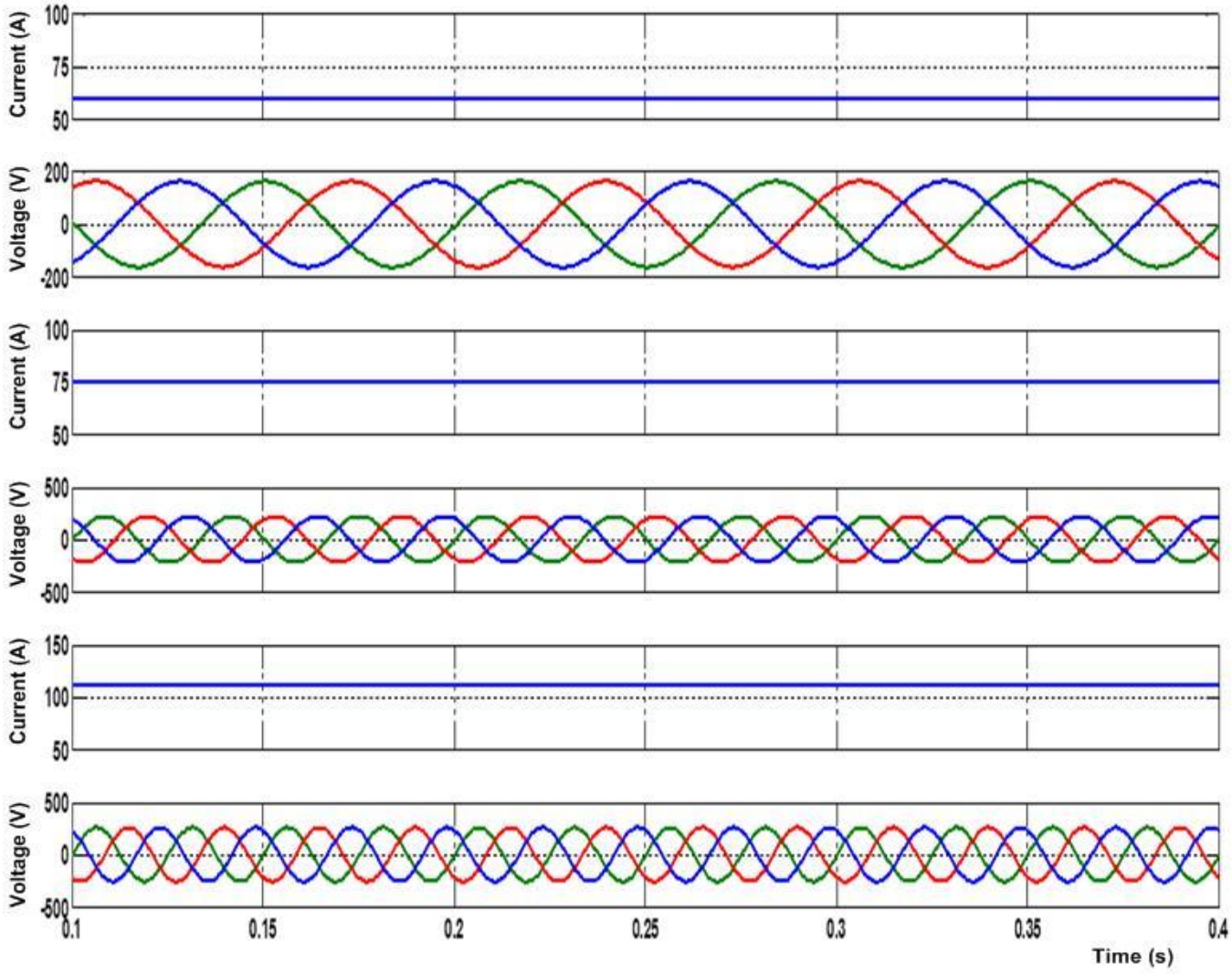


**Fig 13.** Voltage and current waveforms of PMSG at different velocities (a) at 5 m/s, (b) at 10 m/s, (c) at 12 m/s

DDWECS simulations using an MPPT controller are displayed in Table 2 as simulated readings. With wind speeds of 5 meters per second and a rotational speed of 99 revolutions per minute, it is noted from the simulation results that 262 watts are the highest power collected. The wind turbine with PMSG's predicted waveforms at various wind velocities is shown in Fig. 13. Fig 14 shows the corresponding ZSI output voltages. From the waveforms, it is identified that the ZSI terminal voltage is maintained constant by timely alternating the shoot-through duty ratio of the ZSI. The proposed wind turbine generator works in the maximum power point region after implementing the MPPT controller. It is noted that the proposed control strategy shows an immediate follow-up of the maximum power point during the rise in wind speed from 6 to 8 m/s, but the traditional algorithm provides a slow response to the maximum power for the change in wind speed. Figs.15 MPPT response for rapid change in wind velocity (a)-(c) demonstrates the complex reaction to abrupt changes in wind velocity of the proposed WECS. The active and reactive powers fluctuate and eventually achieve a stable state. The sensor less MPPT controller determines the optimal rotor speed to monitor maximum power and maintain the output voltage. The analysis and simulation have shown that the proposed MPPT controller has satisfied the objective of extracting maximum power at any wind speed. The proposed MPPT algorithm is 0.05sec faster than the existing method and also the power extraction is around 25 watts greater than the existing MPPT method.

**Table 1:** PMSG generated voltages for different wind speeds

| S.No | Wind Velocity (m/s) | PMSG Output voltage (V) | Generator speed (rpm) |
|---|---|---|---|
| 1 | 3 | 75 | 68 |
| 2 | 4 | 136 | 75 |
| 3 | 5 | 165 | 99 |
| 4 | 7 | 188 | 120 |
| 5 | 8 | 245 | 147 |
| 6 | 10 | 275 | 165 |

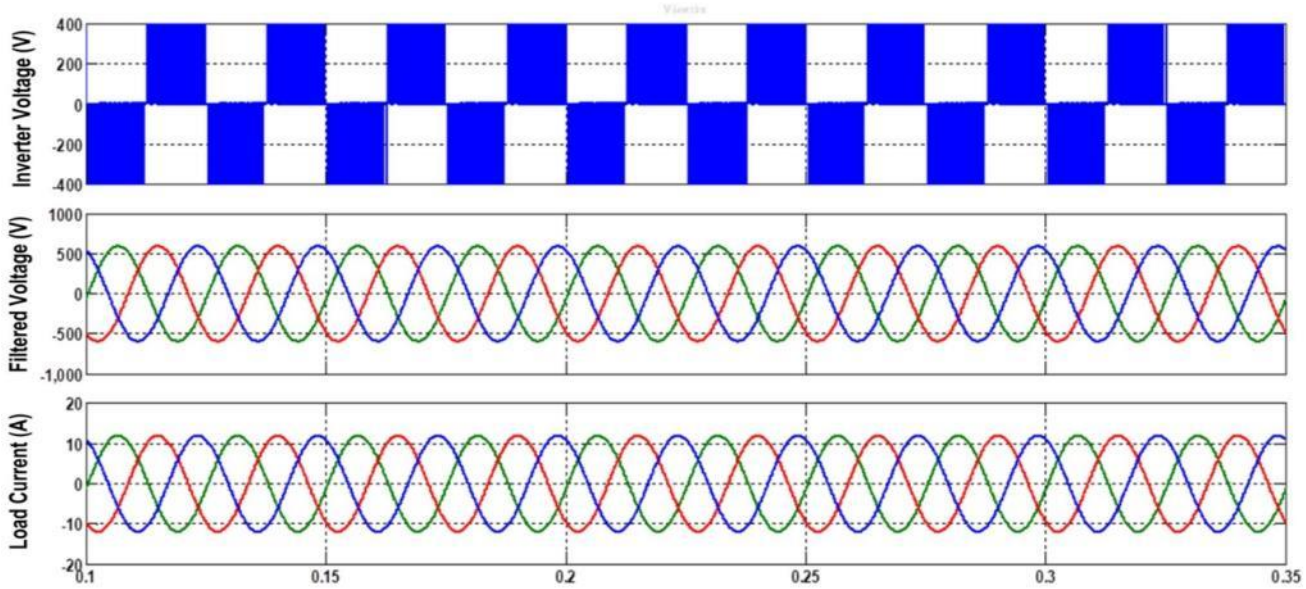


**Fig 14** .ZSI output voltage and current waveforms (a) Terminal Voltage of ZSI , (b) ZSI Voltage with filter (c) Load current

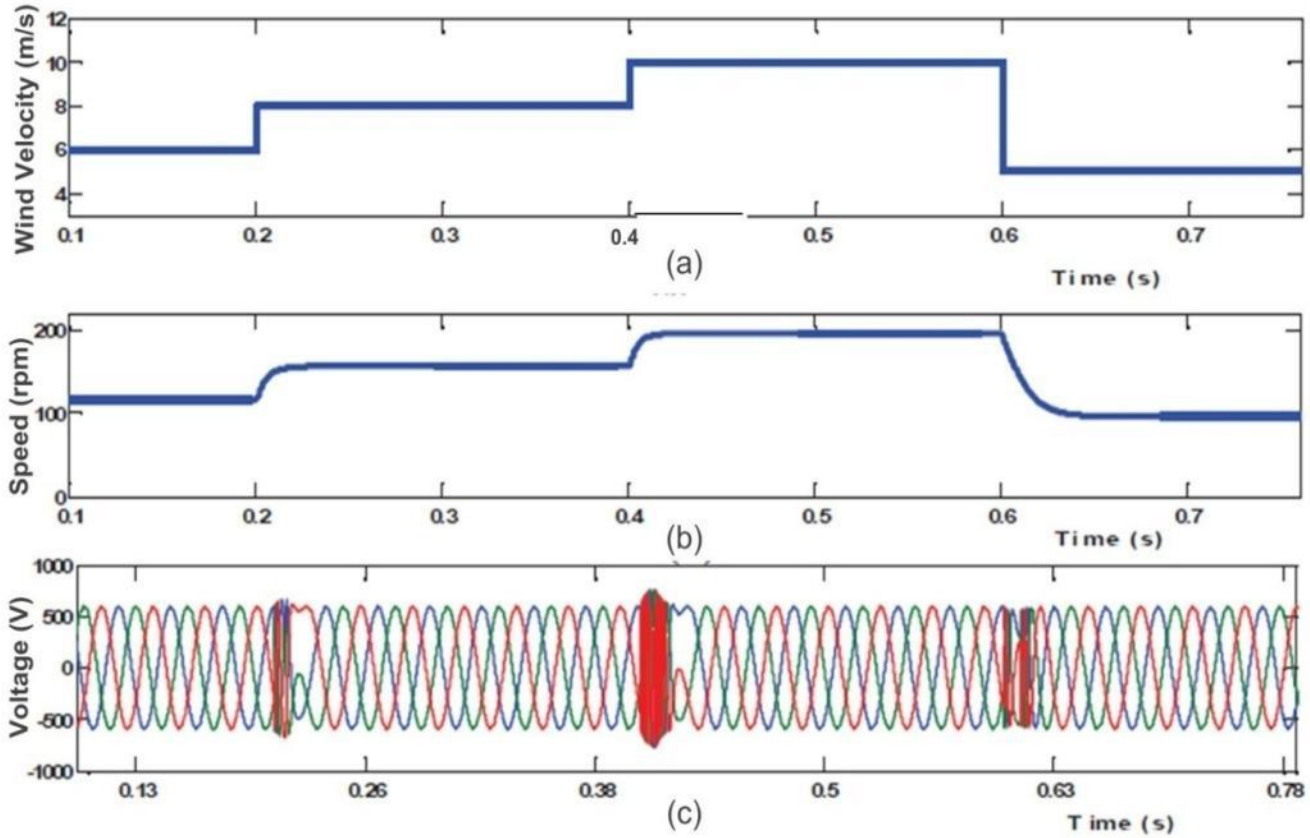


**Fig 15.** MPPT response for rapid change in wind velocity (a)Wind velocity (b) Generated speed (c) Filtered ZSI voltage

## 5. Performance Analysis

The performance analysis of Z-Source Inverter for two types of PWM switching schemes is discussed here. The ZSI performance is analyzed for various values of PMSG generated voltage and different loading conditions. This is done to predict the suitable PWM scheme for ZSI. For comparison analysis, shoot through placement, voltage gain, switching stress and input and output THD are taken into consideration. Table 2 gives the simulation readings of ZSI boost factor and modulation index with three different PWM schemes for different values of PMSG generated voltage.

Table.2 variation of shoot through duty ratio in three PMSG generated voltages.

| S. No | Wind velocity (m/s) | PMSG output voltage (V) | Simple Boost PWM [39] | | THI | | SVPWM | |
|---|---|---|---|---|---|---|---|---|
| | | | Shoot through duty ratio | Boost factor | Shoot through duty ratio | Boost factor | Shoot through duty ratio | Boost factor |
| 1 | 3 | 75 | 0.34 | 4.2 | 0.38 | 4.5 | 0.44 | 4.35 |
| 2 | 4 | 136 | 0.26 | 2.1 | 0.275 | 2.3 | 0.38 | 2.05 |
| 3 | 5 | 165 | 0.16 | 1.47 | 0.176 | 1.55 | 0.34 | 1.55 |
| 4 | 7 | 188 | 0.146 | 1.38 | 0.145 | 1.40 | 0.32 | 1.40 |
| 5 | 8 | 245 | 0 | 0.98 | 0 | 1 | 0 | 1 |
| 6 | 10 | 275 | 0 | 0.98 | 0 | 1 | 0 | 1 |

Table 3: Percentage THD of two different PWM schemes as a function of load power

| Load power (kW) | Simple Boost PWM [39] | | THI | | SVPWM | |
|---|---|---|---|---|---|---|
| | Input current THD (%) | Output voltage THD (%) | Input current THD (%) | Output voltage THD (%) | Input current THD (%) | Output voltage THD (%) |
| 0.25 | 32.2 | 12.62 | 25.5 | 11.55 | 21.4 | 7.75 |
| 0.5 | 28.8 | 14.83 | 28.9 | 14.52 | 26.8 | 8.42 |
| 0.75 | 33.2 | 18.04 | 32.5 | 17.28 | 30.9 | 9.35 |
| 1 | 37.6 | 18.91 | 38.5 | 18.76 | 34.42 | 10.56 |

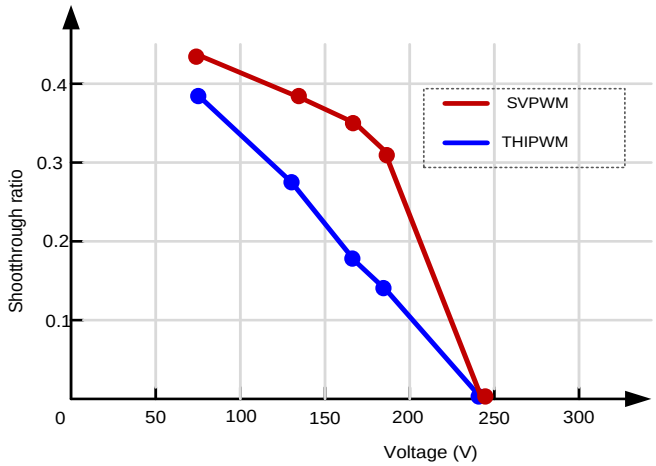


**Fig 16.** Variation of boost factor of ZSI PWM Schemes with variation in PMSG voltage

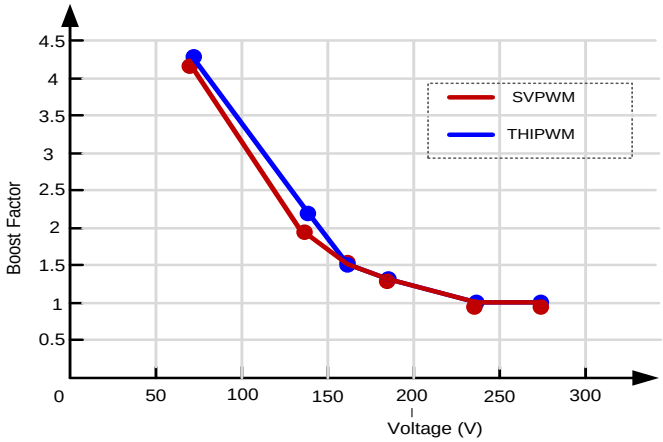


**Fig 17.** Variation of ZSI boost factor with variation in PMSG voltage

The shoot through placement in each PWM scheme is adjusted according to input voltage variation. From Fig 16, it is observed that the variation of shoot through duty ratio $D_0$ in the THIPWM scheme is lesser than in the SVPWM scheme. Fig 17 shows the corresponding variations of boost factor of ZSI for different values of PMSG generated voltage. Table 3 gives the simulated readings for variations in input current and output voltage Total Harmonic Distortion of Z-Source inverter under different PWM schemes with variations in load power. For 1kW load, the SVPWM based ZSI has the input current harmonic distortion of 34.42% and output voltage harmonic distortion of 10.56% whereas they are 37.6 %, 38.5% and 18.91%, 18.76% in the simple boost PWM THI PWM scheme.

## 6. Conclusion

This study review provides the maximum power point tracking algorithm for ZSI-based DDWECSs, PMSG with more pole pairs and the basic operating modes of Z-Source inverter for direct-drive wind energy conversion system with its equivalent circuits were briefly explained. To reduce these power conversion stages and to overcome the limitations of conventional systems, the ZSI based DDWECS is introduced. In this system, the distribution of shoot through periods in two PWM control methods with ZSI, such as maximum boost with THI and MSVPWM is carried out. A comparative study is done between the MSVPWM and THIPWM. It is found that the MSVPWM places the shoot through period faster. MSVPWM reduces voltage ripples by 15V and reduces input current THD by

3.6% and output voltage THD by 7.8%. The THI-based ZSI system has decreased switching stress across the power switches for varying shoot through the duration. The MSPVWM is superior at managing THD and shoot-through period than the ZSI.

**References**

[1] E.P.P.S. Ramos, L.D.O. Assís, R.S. Mena, P.G. Triviño, C.A.G. Vázquez and L.M.F. Ramírez, "Averaged Dynamic Modeling and Control of a Quasi-Z-Source Inverter for Wind Power Applications," IEEE Access, Vol. 9, pp. 114348-114358, 2021.

[2] S.M. Barakati, J.D. Aplevich, and M. Kazerani, "Controller design for a wind turbine system including a matrix converter," Proceedings of IEEE Power Engineering Society, General Meeting, pp. 1-8, 2007.

[3] Z. Wu, Y. Iida and Y. Uematsu, "The flow fields generated by stationary and travelling downbursts and resultant wind load effects on transmission line structural system," Journal of Wind Engineering and Industrial Aerodynamics, DOI:10.1016/j.jweia.2021.104521, Vol. 210, pp. 1-15, 2021.

[4] Y. Zhang, S. Huang, S. Hu, "Ride-through strategy of quasi-Z-source wind power generation system under the asymmetrical grid voltage fault," IET Electric Power Applications. Vol.11, pp. 504–511, 2017.

[5] M. Kesraoui, N. Korichi, and A. Belkadi, "Maximum power point tracker of wind energy conversion system," Renewable Energy, Vol.36, No.11, pp. 2655-2662, 2011.

[6] Z.P. Fang, "Z-Source Inverter," IEEE Transactions on Industry Applications, Vol. 39, No.2, pp. 504-510, 2003.

[7] M.A.H. Navas, G.F. Lozada, J.L.A. Puma, A.J.A. Torrico and A.J.S. Filho, "Battery Energy Storage System Applied to Wind Power System Based On Z-Source Inverter Connected to Grid," IEEE Latin America Transactions, Vol. 14, No. 9, pp. 4035-4042, Sept. 2016.

[8] J. Li, J. Liu, and L. Zeng, "Comparison of Z-Source Inverter and Traditional Two Stage Boost-Buck Inverter in Grid-tied Renewable Energy Generation," IEEE 6th International Conference on Power Electronics and Motion Control, pp.1493-1497, 2009.

[9] K.V. Bhadane, M.S. Ballal, A. Nayyar, D.P. Patil, T.H. Jaware and H.P. Shukla, "A Comprehensive Study of Harmonic Pollution in Large Penetrated Grid-Connected Wind Farm," Mapan - Journal of Metrology Society of India, DOI:10.1007/s12647-020-00407-z, Vol.36, pp. 729–749, 2021.

[10] S. Rajakaruna, Y. Jayawickrama, and N. Maw, "Steady-State Analysis and Designing Impedance Network of Z-Source Inverters," IEEE Transactions on Industrial Electronics, Vol.57, No.7, pp. 2483-2491, 2010.

[11] A. Chub, O. Husev, A. Blinov and D. Vinnikov, "Novel Isolated Power Conditioning Unit for Micro Wind Turbine Applications," IEEE Transactions on Industrial Electronics. Vol. 64, pp. 5984–5993, 2017.

[12] R. Bharanikumar, "Certain Investigations on Direct Drive Wind Energy Conversion System with Reduced Stage Power Conversion using Z-Source Inverter and Matrix Converter," Ph.D. Thesis, Anna University Chennai, India, 2012.

[13] Ch. R. Reddy, K. Naresh, P.U. Reddy and P Sujatha, "Control of DFIG Based Wind Turbine with Hybrid Controllers," International Journal of Renewable Energy Research, Vol. 10, No. 3, pp. 1488-1500, 2020.

[14] Y. Zhang, Z. Cheng, Q. Chen and Q. Li, "An Enhanced Half-Quasi- Z -Source Inverter for Wind Energy Conversion System with D-PMSG" Complexity, doi:10.1155/2021/9962115, Vol. 2021, pp. 1-15, 2021.

[15] R.I. Putri, F. Ronilaya, I.N. Syamsiana, "Maximum Power Extraction For Hybrid Solar Wind Renewable Energy System Based on Swarm Optimization," International Journal of Renewable Energy Research, DOI: 10.20508/ijrer.v11i3.12161.g8253, Vol. 11, No. 3, pp. 1215-1222, 2021.

[16] Y. Nima, S.H. Fathi, N. Farokhina and H.A. Abyaneh, "THD Minimization Applied Directly on the Line-to-Line Voltage of Multilevel Inverters," IEEE Transactions on Industrial Electronics, Vol.59, No.1, pp.373-380, 2012.

[17] E. Vani and N. Rengarajan, "Reduction of harmonics in a wind power conversion system by the optimal function of a Vienna rectifier and switched inductance Z source inverter," Research Journal of Biotechnology, Vol. 2017, No. 2, pp. 188–198, 2017.

[18] V. Agarwal, R.K. Aggarwal, P. Patidar and C. Patki, "A Novel Scheme For Rapid Tracking of Maximum Power Point in Wind Energy Generation Systems," IEEE Transactions on Energy Conversion, Vol. 25, No. 1, pp. 228-236, 2010.

[19] S.Y. Zhang, S. Huang, D. Luo, "A Novel Half Quasi-Z-source Inverter for Wind Energy Conversion Systems," Zhongguo Dianji Gongcheng Xuebao/ Proceedings of the Chinese Society of Electrical Engineering, Vol.37, pp. 5107–5117, 2017.

[20] Y. Liu, B. Ge, A. Haitham and F.Z. Peng, "A modular multilevel space vector modulation for photovoltaic quasi-z-source cascade multilevel inverter," Twenty-Eighth Annual IEEE Applied Power Electronics Conference and Exposition (APEC), California, pp. 714-718. 2013.

[21] R. Dehghanzadeh, V. Behjat, M. R. Banaei, "Dynamic modeling of wind turbine based axial flux permanent magnetic synchronous generator connected to the grid with switch reduced converter," Ain Shams Engineering Journal, Vol. 9, No. 1, pp. 125–135,2018.

[22] S. A. Saleh and R. Ahshan, "Resolution-Level-Controlled WM Inverter for PMG-Based Wind Energy Conversion System," IEEE Transactions on Industry Applications, Vol. 48, No. 2, pp. 750-763, March-April 2012.

[23] E.P.P.S. Ramos, L. de O. Assis, R. Sarrias, P. García, C.A. García and L.M. Fernández, "Large-Scale Wind Turbine With Quasi-Z-Source Inverter and Battery," 22nd IEEE International Conference on Industrial Technology (ICIT), Valencia, pp. 403-408, 10-12 March 2021.

[24] Y. Li, S. Jiang, G.J. Cintron, and F.Z. Peng, "Modeling and Control of Quasi-Z- Source Inverter for Distributed Generation Applications," IEEE Transactions on Industrial Electronics, Vol. 60, No.4. 2013.

[25] Y. Liu, B. Ge, H. Abu and F.Z. Peng, "Impedance design of 21-kW quasi-z-source H-bridge module for MW-scale medium-voltage cascaded multilevel photovoltaic inverter," 2014 IEEE 23rd International Symposium on Industrial Electronics (ISIE), Istanbul, Turkey, pp. 2490-2495, 1-4 June 2014.

[26] S. Bayhan, H. Abu-Rub and R. S. Balog, "Model Predictive Control of Quasi-Z-Source Four-Leg Inverter," IEEE Transactions on Industrial Electronics, Vol. 63, No. 7, pp. 4506-4516, July 2016.

[27] Y. Li, F. Z. Peng, J. G. Cintron-Rivera and S. Jiang, "Controller design for quasi-Z-source inverter in photovoltaic systems," 2010 IEEE Energy Conversion Congress and Exposition, Atlanta, GA, USA, pp. 3187-3194, 12-16 Sept. 2010.

[28] S. Fitzgerald, R. Kelso, P. Grimshaw, A. Warr, "Observations of the flow experienced by a track cyclist using velodrome, wind tunnel, and potential flow investigations with an instrumented bicycle," Journal of Wind Engineering and Industrial Aerodynamics, DOI:10.1016/j.jweia.2020.104374, Vol. 206, pp. 1-12, Nov 2020.

[29] Y. Liu, B. Ge, F. J. T. E. Ferreira, A. T. de Almeida and H. Abu-Rub, "Modeling and SVPWM control of quasi-Z-source inverter," 11th International Conference on Electrical Power Quality and Utilisation, Lisbon, Portugal, pp. 1-7, 17-19 Oct. 2011.

[30] N. Priyadarshi, S. Padmanaban, D. M. Ionel, L. Mihet-Popa and F. Azam, "Hybrid PV-Wind, micro-grid development using quasi-Z-source inverter modeling and control-experimental investigation," Energies, DOI:10.3390/en11092277, Vol. 11, No. 9, pp. 1-15, 2018.

[31] R. Datta and V. T. Ranganathan, "A method of tracking the peak power points for a variable speed wind energy conversion system," IEEE Transactions on Energy Conversion, vol. 18, no. 1, pp. 163-168, March 2003.

[32] H. Li, and Z. Chen, "Design optimization and site matching of direct-drive permanent magnet wind power generator systems," Renewable Energy, Elsevier, Vol. 34, No. 4, pp. 1175-1184, 2009.

[33] P. Fernandez, F.D. Reijedo, A. Vidal, A.G. Yepes, J. Malvar, O. Lopez, A. Nogueiras and J.D Gandoy "A Signal Processing Adaptive Algorithm for Selective Current Harmonic Cancellation in Active Power Filters," IEEE International Symposium on Industrial Electronics, Vol. 56, pp. 2946- 2951, 2010.

[34] F. Wang, Y. Zhang and Y. Shen, "Comparison of different structures for variable speed constant frequency wind power generator," 2008 International Conference on Electrical Machines and Systems, Wuhan, pp. 2234-2238, 17-20 Oct. 2008.

[35] D. Ghaderi, S. Padmanaban, P. K. Maroti, B. Papari, J. and B. Holm-Nielsen, "Design and implementation of an improved sinusoidal controller for a two-phase enhanced impedance source boost inverter," Computers and Electrical Engineering, DOI: 10.1016/j.compeleceng.2020.106575, Vol. 83, ,pp. 1-18, May 2020.

[36] D.C. Meena, M. Singh, A.K. Giri, "A Modified NLMS Control Algorithm for Coordinated Operation in Three-Phase Wind-Energy Conversion System", International Journal of Renewable Energy Research, DOI: 10.20508/ijrer.v11i4.12454.g8344, Vol. 11, No. 4, pp.1621-1629, 2021.

[37] V. F. Pires, D. Foito, A. Cordeiro and A. J. Pires, "A Bidirectional DC-DC Converter to Interlink Unipolar and Bipolar DC Microgrids," 2021 9th International Conference on Smart Grid (icSmartGrid), Setubal, Portugal, pp. 37-42, 29 June-1 July 2021.

[38] A. Radwan, I. Khouri and X. Jiang, "Modeling and Control of Current-Source Converter-Based AC Microgrids," 2020 IEEE 8th International Conference on Smart Energy Grid Engineering (SEGE), Oshawa, Canada, pp. 97-101, 12-14 Aug. 2020.

[39] A. Belkaid, I. Colak, K. Kayisli and R. Bayindir, "Design and Implementation of a Cuk Converter Controlled by a Direct Duty Cycle INC-MPPT in PV Battery System," International Journal of Smart Grid, DOI: 10.20508/ijsmartgrid.v3i1.37.g42, Vol 3, No 1, pp. 1-7 , 2019.

[40] V. Mishra, R.D. Shukla, P. Gupta, "An Approach towards Application of Semiconductor Electronics Converters in Autonomous DFIM Based Wind Energy Generation System: A Review," International Journal of Smart Grid, DOI: 10.20508/ijsmartgrid. v3i3.69.g61, Vol 3, No 3, pp. 1-11 , 2019.

[41] M. Quraan, Q. Farhat and M. Bornat, "A new control scheme of back-to-back converter for wind energy technology," 2017 IEEE 6th International Conference on Renewable Energy Research and Applications (ICRERA), San Diego, USA, pp. 354-358, 5-8 Nov 2017.

[42] K. Kajiwara, R. Daimon, Y. Ohta, A. Segami, N. Matsui and F. Kurokawa, "Voltage Balance of Multiconnected Half Bridge Converter," 2021 10th International Conference on Renewable Energy Research and Application (ICRERA), Istanbul, Turkey, pp. 439-442, 26-29 Sept. 2021.